Group Project Report

Brain Tumor Classification
using deep learning

Project Members

BI12-359 Nguyen Ha Phuong
BI12-423 Nguyen Thi Thao
BI12-462 Nguyen Cam Tu
BI12-061 Pham Ha Chau
BI12-190 Vu Phuc Hung
BI12-175 Pham Minh Hoang

A report presented for the course
BI12| DS

ICT Department
University of Science and Technology of Hanoi

April 6, 2024

Contents

Keywords: Brain Tumor, Deep Learning, Supervised Learning, MRI

1 Introduction

1.1 Why do we choose this topic ?

The brain, a body part that looks inside for purpose and meaning, is the hub of the nervous system, which regulates all other bodily organs. Thus, every brain abnormality has the potential to be harmful to human health. The most serious of these anomalies are cerebral bleeding, hydrocephalus, and brain tumors. There are two types of brain tumors: primary and secondary (secondary). Primary brain tumors that originate from the brain's cells can either be benign or malignant. When malignant cells from another region of the body move to the brain, secondary brain tumors happen. While secondary tumors spread from other regions of the body into the brain through movement, primary tumors are found in the brain tissue [1]. The World Health Organization (WHO) has classified brain tumors into four classes. Tumors classified as grade 1 or grade 2 refer to lower-grade tumors (like meningiomas), whereas grade 3 and grade 4 tumors are made up of more severe ones (like gliomas). Meningioma, pituitary, and glioma tumor incidence rates in clinical practice are around 15%, 15%, and 45%, respectively [2]. A battery of neurological and physical tests is used to diagnose brain tumors. Utilizing MR (Magnetic Resonance) and CT (Computerized Tomography) for diagnosis, pathological assessment and biopsy are carried out to validate the diagnosis. Since MR is the only non-invasive and non-ionizing imaging mode among them all, it is regarded as the most desirable modality [3].

Using current resources and real-world requirements, I have selected the topic "Brain tumor classification using deep learning."

To improve patient survival rates, our effort aims to assist healthcare professionals—especially those lacking considerable expertise—and facilitate prompt patient diagnosis. By concentrating on brain tumors, this study seeks to support a more general objective: the growth of artificial intelligence and medicine through the application of technology in healthcare, which will ultimately benefit society. In addition to addressing particular problems in the medical profession, the study also impacts worldwide goals, encouraging fair and creative advancement in deep learning's field.

1.2 The purpose of this work

We established the following primary goals for this study:

- Create several types of deep learning models, such as VGG16, Inception V3, and so on, with the express purpose of accurately identifying photos of brain tumors.
- Take into account the complexity and diversity of brain disorders, improving the model's capacity to adapt to changes in disease patterns and provide precise diagnoses for a range of ailments.
- Outperform current models in the field of brain tumor classification with high accuracy and improved efficacy.

1.3 Object and scope of the study

The use and integration of convolutional neural networks (CNNs) for the job of brain tumor detection is the main emphasis of this work. The research's scope includes every step of developing a system for identifying brain tumors, including data collection, preprocessing, model creation, training, assessment, and result analysis. Testing different architectural options, training plans, and performance measures are all part of the research to determine the best method for identifying brain tumors.

1.4 Research methods

This method is constructed using thorough and methodical elements, such as:

- Thorough gathering of data including locating pictures of brain tumors, then we put data through augmentation, and normalization to get ready for training.
- Creating and implementing Inception V3 and VGG16 models, which combine CNN feature extraction capabilities.
- Applying optimization methods, strict training regimens, and meticulous hyperparameter tweaking.
- Assessing using industry-standard measures.

1.5 The format of this work

The format of the work is as follows. Related works are given in Section 2. In Section 3, some fundamental methods are presented. In Section 4, we present the experiments of methods and the results. In Section 5, the paper is finally concluded.

2 Related works

Various techniques had been proposed in previous years for segmentation and classification. These methods made use of deep learning models [4] and conventional machine learning [5]. We have examined this portion of the literature used to categorize brain tumors. Jude Hemanth et al. [6] address the ANN's convergence period disadvantages in their study to provide a model for MRI-based brain abnormality identification. Their primary goal in creating this model was to construct two modified versions of the CPN (Counter Propagation Neural Model) and KNN (Kohonen Neural Network), which they named MCPN and MKNN, respectively. The idea is to adapt the ANN model so that it can solve the convergence rate. They were able to accomplish this, and the accuracy rate after modification is 95% for MKNN and 98% for MCPN.

The authors of Paul et al.'s [7] proposal for two neural network models—a fully connected neural network and a convolution neural network—perform classification using a dataset that has three classes, each of which is divided into three separate planes. To ensure that the model performs accurately, the authors test it by choosing only the axial plane. They note that a basic model like the one that has been suggested can outperform those specialist approaches and that CNN performs better with an accuracy

of 91.43%. Using this method, Afshar et al. [8] suggest a member network capsule (CapsNet), an enhanced CNN architecture for classifying brain tumors. CapsNet is a method that utilizes the spatial interaction between the tumor and surrounding tissues. The highest accuracy of the segmented tumor and the raw brain picture was 86.56 percent and 72.13 percent, respectively.

Abiwinanda et al.'s [9] proposal is to investigate the basic CNN model without making any changes—rather, only working with CNN and adjusting the number of its various layers. They created seven distinct CNN designs in this manner, varying in the number of layers in each, and concluded that the second architecture—which has two layers in each convolution, activation, and max pooling—proves to be the best of all, yielding a training accuracy of 98.51%.

Lin et al. [10] have suggested more studies to categorize meningioma tumors into several grades. Slow-growing tumors classified as non-cancerous are found in Grade I. Both malignant and noncancerous tumors are found in grade-II. There are malignant tumors in grade-III that have a rapid growth rate. As contextual and radiological characteristics, many features are used. There is no preprocessing or segmentation done. Multiple logistic regression was employed by the authors in the classification stage. Using MRI scans from 120 patients—90 with Grade I and 30 with Grade II or III—the suggested plan is evaluated. They made use of T1 and T2 in FLAIR, among other sequences. Feature extraction is done via DWI transformation. With the utilized dataset, the findings are satisfactory. To guarantee the validity of this type of approach, several huge datasets are necessary.

Ghassemi et al. [11] have also reported using CNN on this dataset to develop a novel model for multi-class brain tumor classification. To extract significant features, the model is first pre-trained as a discriminator in a generative adversarial network (GAN). To distinguish between three cancers, a SoftMax classifier was then inserted instead of the final fully linked layer. There are six levels in the suggested model. It was applied using several methods of data augmentation. Its accuracy on the introduced and random splits was 95.6% and 93.01%, respectively.

Sachdeva et al. [48] have proposed a semi-automatic classification approach with a variety of phases to aid radiologists in classifying MRIs. To identify tumor regions, the first step involves using a content-based active contour system that enables the radiologist to manually identify the region of interest (ROI), which is then stored as a segmented ROI (SROI). Next, the SROI is used to extract 71 texture and intensity characteristics. Ideal

The Genetic Algorithm (GA) is used to carry out feature selection. SVM and ANN are the two classifiers used in the last phase to classify the selected characteristics. The proposed approach is evaluated using various datasets. Sachdeva et al. [12] have proposed a semi-automatic classification approach with a variety of phases to aid radiologists in classifying MRIs. Using a content-based active contour system, the radiologist may manually choose the region of interest (ROI) and store it as a segmented ROI (SROI) in order to identify tumor locations. Next, the SROI is used to extract 71 texture and intensity characteristics. The Genetic Algorithm (GA) is used to choose features in the best possible way. SVM and ANN are the two classifiers used in the last phase to classify the selected characteristics. Several datasets are used to test the recommended method. There are 428 MR pictures in the first dataset and 260 in the second. Six tumor classifications are shown in the first set of images: Glioblas-

toma Multiforme (GBM), Meningioma (MEN), Astrocytoma (AS), Medulloblastoma (MED), pediatric tumor, and secondary tumor-metastatic (MET). There are just three tumor classifications in the second dataset: AS, MEN, and Low-Grade Glioma. While GA-ANN seeks to confirm the correctness, the proposed GA-SVM seeks to find a preliminary probability for the tumor category. According to the performance analysis performed on the initial set of pictures, the GA-based technique increased ANN accuracy to 94.9% and SVM accuracy to 91.7%. SVM accuracy increased to 89% in the second set of pictures, and 94.1% for ANN. The findings show that in comparison to GA-SVM, the classifier GA-ANN produced the best results. Additionally, GA-ANN gives accuracy whilst GA-SVM yields speed. The results show that the proposed approach performs satisfactorily and can help radiologists make better decisions when it comes to classifying brain cancers.

3 Methodology

3.1 Our model

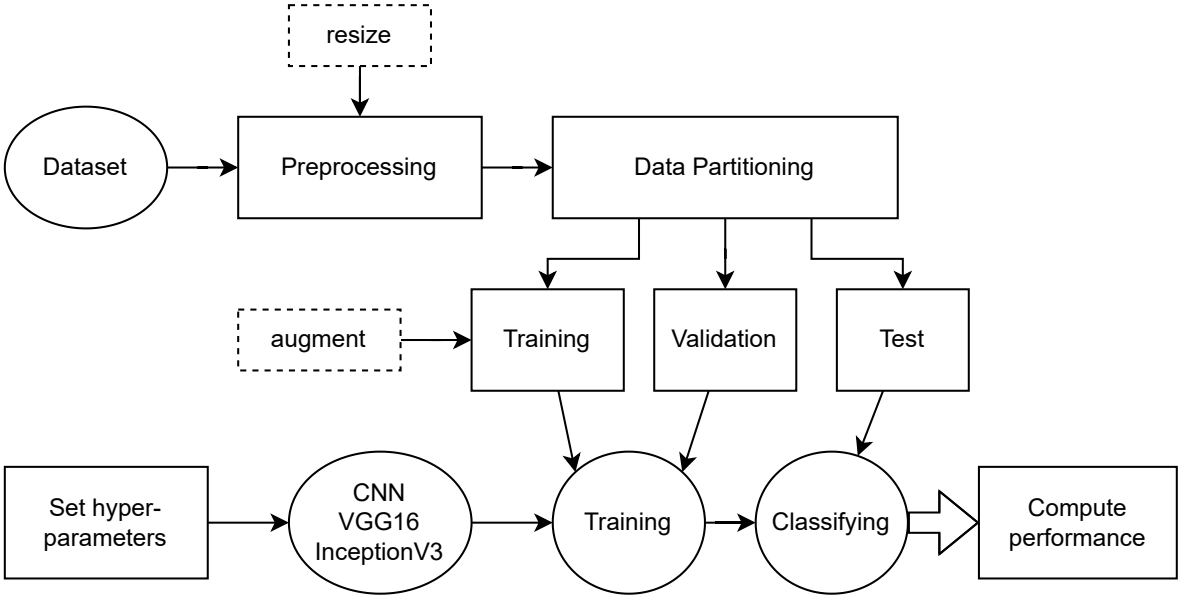

Figure 1: The pipeline of our model

Figure 1 shows the pipeline of the proposed method, starting with the system loading the images. These images have been labeled and categorized into 4 classes, then go through the pre-processing step to be resized. Next, the system makes an augmentation technique after splitting the dataset into training, validation, and test sets. Now, we will introduce the structure of our model/ customed VGG16 mode/ customed InceptionV3 model, which has been set hyper-parameters. Finally, we complete the training and compute performance.

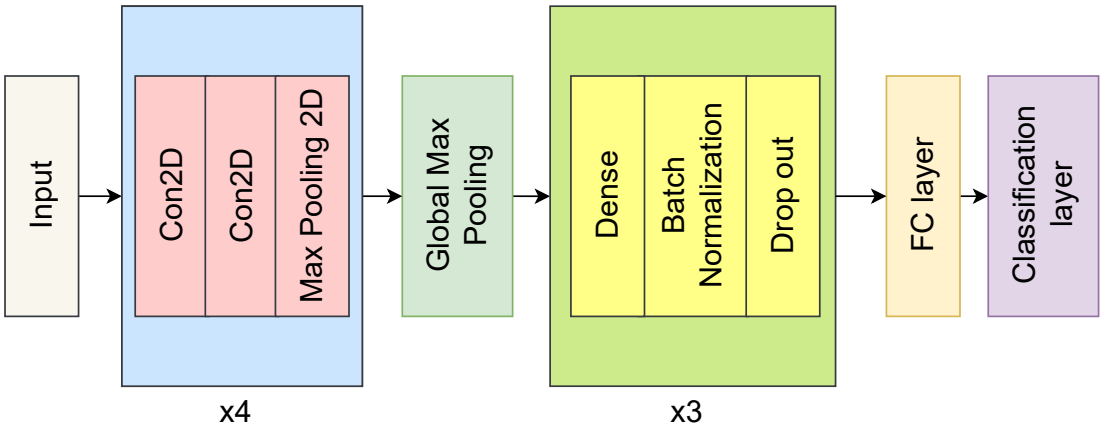

Figure 2: The architecture of our model

This figure shows the proposed convolutional neural network (CNN) structure using the Sequential API in Keras. It includes many layers starting from the input layer with images extracting features and then fully connected layers for classification.

The input layer comes first and only accepts shape images (256, 256, 3). Secondly, the structure consists of several convolutional layer pairs, each having 64, 128 256, and 512 filters. In each convolutional layer, ReLU activation function, 'same' padding, and a kernel size of (3, 3) are used. After that, we spatially downsample the feature maps using a pooling window of size (2, 2). In addition, we combine the spatial data from many feature maps into a single vector using the GlobalMaxPooling2D layer. The fully connected layers come next, having three dense layers with 256, 128, and 64 neurons each. To avoid overfitting, these levels are followed by batch normalization and dropout layers. Finally, we have a classification layer with a softmax activation function. We apply the Adam optimizer, a categorical cross-entropy loss function, an accuracy metric, and a learning rate of 0.0001 for the compilation.

3.2 VGG16

In this work, CNN is used in conjunction with the VGG-16 architectural model for model training. CNN is a two-dimensional data processing enhancement of the Multilayer Perceptron. Since CNN has a high network density and is frequently employed with picture data, it is inherent to Deep Neural Networks [13]. The feature extraction layer and classification layer are the two primary layers of the CNN technique. Convolutional layers, RelU activation layers, and pooling layers applied to the input image make up the input of the feature extraction layer. Subsequently, fully linked layers and softmax activation layers are included in the classification layer.

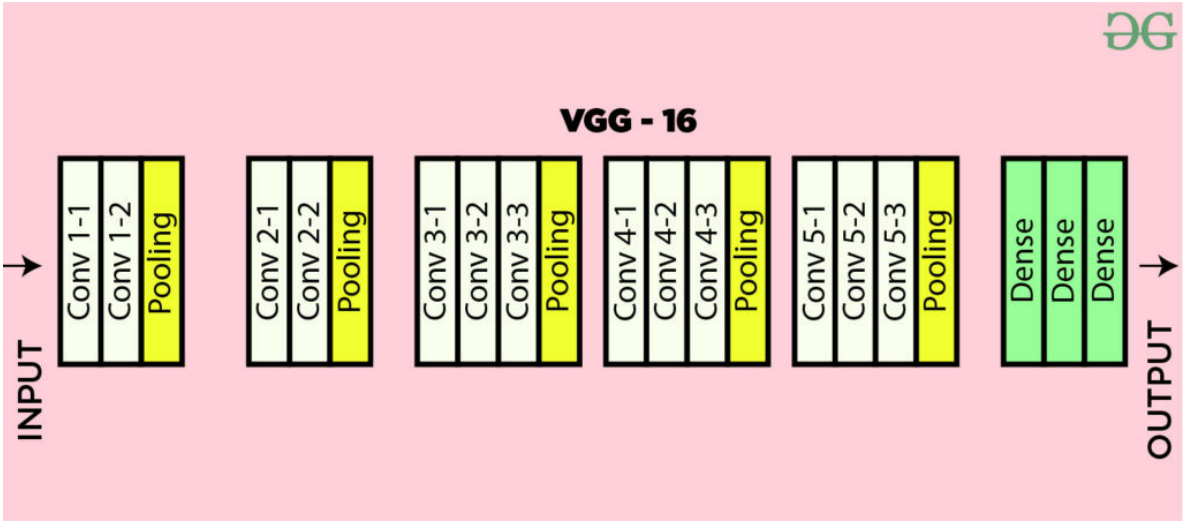

Figure 3: The architecture of VGG16

By calculating the effectiveness of the classification process and using specific parameters to balance the classification findings, a confusion matrix is a useful tool. The classification performance measurement results using the confusion matrix are represented by four terms. Total False Positive (TFP), Total True Negative (TTN), Total True Positive (TTP), and Total False Negative (TFN) are some of them. Accuracy, precision, recall, and f1-score values can be obtained based on TTP, TTN, TFP, and TFN values [14].

The loss value will be considerable if the model's prediction is off. The loss number will be near the previous amount if the model's forecast is accurate enough. One of the loss functions used to categorize multi-class data is categorical cross-entropy. Put simply, the model has to select one category when there is data that fits into others. Its formal purpose is to quantify the variation between two probabilities [4].

The optimizer is crucial to the CNN model's extensive training process, which involves iteratively updating every layer in the network. One popular method for neural network optimization is gradient descent [5]. The taken-into-consideration parameters are rearranged in the opposite direction as the gradient of the objective function to lower the loss function.

3.3 InceptionV3

Convolutional neural networks (CNNs) are used in Inception V3 for object detection and image analysis. This is version three of Google's Inception CNN, which debuted at the HAM10000 Recognition Challenge. To enhance its performance, Inception V3 employs factorized 7 x 7 convolutions, label smoothing, and an additional classifier. Compared to AlexNet, which has 60 million parameters, it has less than 25 million. On the ImageNet dataset 123, it can attain accuracy levels higher than 78.1%.

The model outperformed previous CNN models like VGG16 and ResUNet 4, with an overall accuracy of 87.6%. In a different study, the effectiveness of three traditional CNN models—VGG-16, VGG-19, and Inception V3—was evaluated using a dataset of 2,000 photos showing three different forms of skin cancer. According to the study, among all the models, Inception V3 had the lowest loss and the highest accuracy.

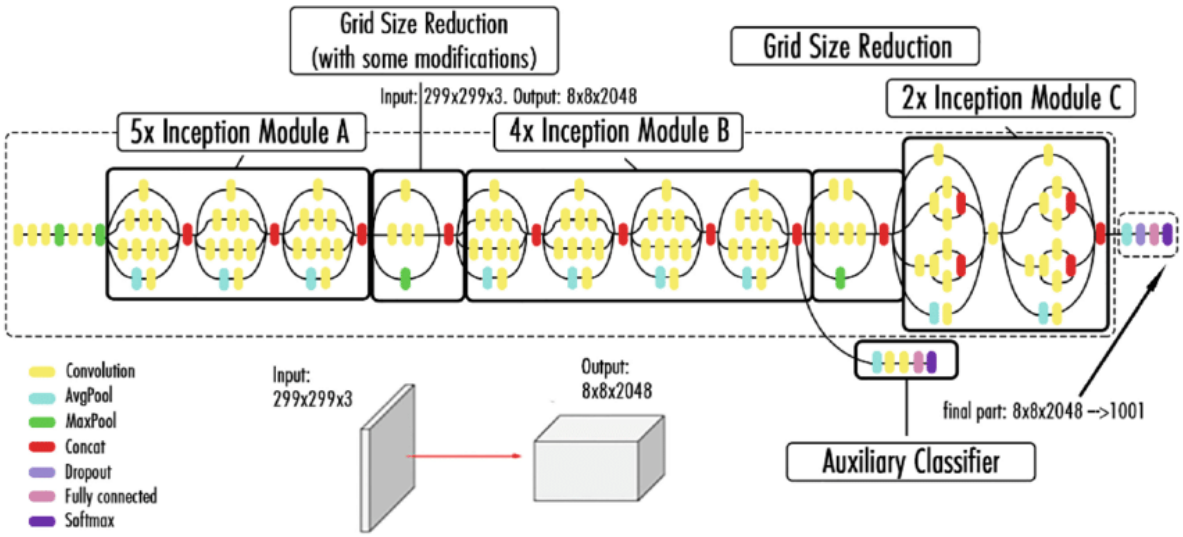

Figure 4: The architecture of InceptionV3.

4 Experiments

4.1 Data Preprocessing

We use a publicly accessible Brain Tumor MRI dataset, which is available on the Kaggle repository for our studies in this publication. There are 7,023 MRI images of the human brain, categorized into 4 classes: glioma, meningioma, pituitary, and no tumor. From random sizes, the images are resized to 256 x 256.

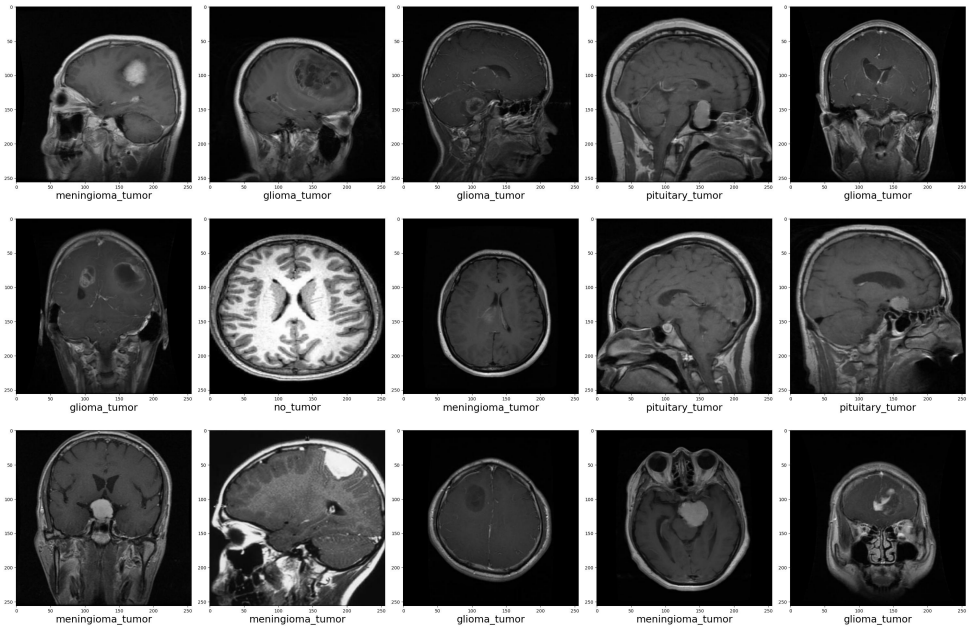

Figure 5: Sample MRI images in the Brain Tumor MRI dataset.

This dataset contains a huge number of images but is still evenly distributed into 4 classes in total and each dataset: training, validation, and test. There were 7,023 photos in the original dataset, 65% training (4,569 images), 15% validation set (1,143 images), and 19% testing set (1,311 images).

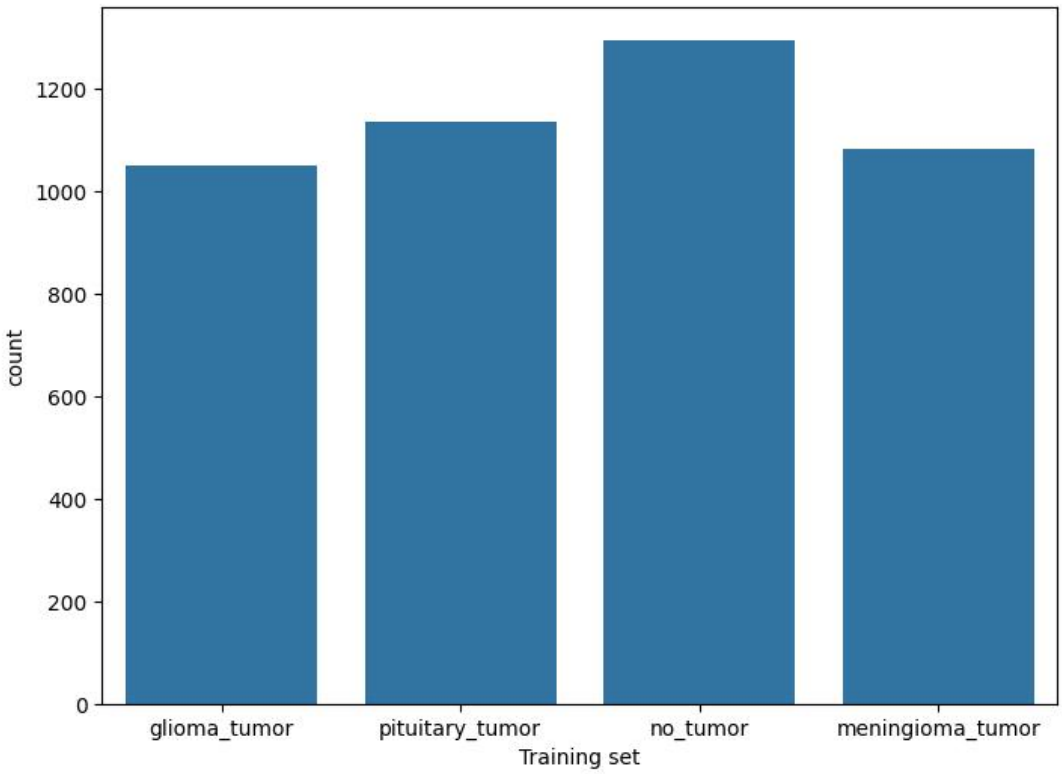

Figure 6: Distribution in training dataset.

Table 1: Counts for each type of brain tumor

Class	**Number of Images**
glioma	1,621
meningioma	1,645
pituitary	1,757
no tumor	2,000
Total	7,023

Despite the equally distributed dataset, the model may confront problems like underfitting or overfitting. Misclassifying disease is a risk for those working in the medical industry.

To overcome the problem, we used data augmentation for the highly skewed dataset, including rotation, width shifting, height shifting, shear, and zoom ranges. A rotation range of 30 degrees allows for random rotations of images within this range. Width

and height shift range shift the image horizontally and vertically in a range of 0.2, respectively. A shear range of 0.2 controls the magnitude of shear transformations applied to the images. Zoom range is zoom in or zoom out the image in a range of 0.2 to create a new image. When these parameters are combined, various transformations may be performed to the training pictures, which improves the model's robustness and ability to generalize.

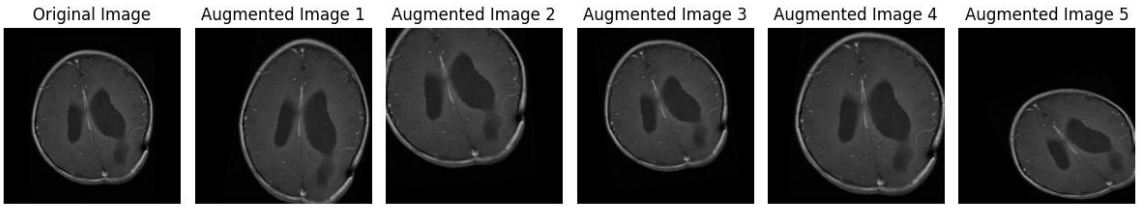

Figure 7: Output after augmenting an image.

4.2 Model Selection and Preprocessing

In this section, we will explain how we have customized different pre-trained models to adapt them to our classification task. We have two models from the Keras library: VGG16 and InceptionV3. These models were pre-trained on the ImageNet dataset containing 1.2 million images of 1000 classes. We removed the original top layers of each model and added new layers suitable for our task, which is to classify images into four categories.

For the VGG16 model, we added a global max pooling layer, batch normalization layers, dense layers with ReLU activation, a dropout layer with 0.5 rate, and 128, 64 units respectively. After that, a final dense layer with 4 units and softmax activation is added. The global max pooling layer reduces the dimensionality of the feature maps and extracts the most salient features. The dense layer adds non-linearity and increases the model's capacity. The dropout layer prevents overfitting by randomly dropping out some units during training. The final dense layer produces the probability distribution over the four classes.

For the InceptionV3 model, we added a global max pooling layer, batch normalization layers, dense layers with ReLU activation, a dropout layer with 0.5, 0.4, 0.3 rate, and 256, 128, 64 units respectively. Lastly, a final dense layer with 4 units and softmax activation is added.

Table 2: Different architectures and hyperparameters tested and tried on our model before the final result

Factor(S)	**Values**
Number of Convolutional + ReLU layers	2,3,4
Batch normalization	1,2,3
Number of drop-out layers	3,4,6
Max epochs	10,20,30,40,50
Number of fully connected layers	2,3,4
Number of convolutional kernels	16,32,64,128
Kernel size	2,3,5,7
Pooling layer	Max pooling, average pooling
Pooling layer window size	2,3
Optimizers	Adam
Mini-batch size	16,32,64
Dropout rate	0.2,0.3,0.4,0.5
Initial learning rate	0.001, 0.0001
Learning rate drop factor	0.5

4.3 Feature Extraction

We will describe how we pre-trained and adjusted the pre-trained models in this part with our dataset to help the model learn meaningful features from our dataset.

Two models were pre-trained for five epochs using a 64-batch batch size. We have utilized Adam optimizer with a learning rate of 0.0001 and epsilon of 1e-7, cross-entropy loss function, and the accuracy metric. We used the fit method of the Keras model class to train the model with the augmented training and validation data, the steps per epoch and validation steps arguments to specify the number of batches per epoch for the training and validation data, respectively.

Before fine-tuning, all the layers of the base model are set to be trainable. This allows the model to learn more specific features from our dataset and improve its performance. We fine-tuned each model for 10 epochs with a batch size of 64. The arguments are the same as in the pre-training phase, except for the callbacks argument. The ReduceLROnPlateau callback to reduce the learning rate by a factor of 0.5 if the validation accuracy did not improve for 3 consecutive epochs, with a minimum learning rate of 1e-7 and a cooldown of 2 epochs. This callback helps to avoid overfitting and find the optimal learning rate for the fine-tuning phase. After the retraining process, we saved the models into Keras files for later use.

Table 3: Parameter table for different models

Model	Parameters	Dropout	Activation	Optimizer	Batch size
VGG16	14M	0.5	ReLU	Adam	64
InceptionV3	22M	0.5	ReLU	Adam	64
Our Model	5M	0.5	ReLU	Adam	64

5 Evaluation and Discussion

5.1 Metrics

Moving on to this section, We will show the metrics used to evaluate the performances on the test data: accuracy, precision, recall, F1-score, and AUC-ROC. We generated the classification of our model and two pre-trained models on the test data using the same procedure as the validation data. The results of our model are displayed in table 4.

$$\text{Accuracy} = \frac{TP + TN}{TP + TN + FP + FN}$$

$$\text{Precision} = \frac{TP}{TP + FP}$$

$$\text{Recall} = \frac{TP}{TP + FN}$$

$$\text{F1-score} = \frac{2 \times Precision \times Recall}{Precision + Recall}$$

where TP is True Positive, FP is False Positive, TN is True Negative, FN is False Negative

5.2 Evaluation

We will provide the results and explanations for our evaluation. The following graphs show the accuracy and the loss of the training and validation of our model after 50 epochs. The first graph shows an increasing trend in the accuracy of the training set during the first 15 epochs, and then a stable result for the rest of the epochs. This suggests the model has learned the features well, not facing over-fitting or under-fitting. In the loss graph, the first 15 epochs reduce the loss significantly. The rest decreases slowly, minimizing the error and converging to a good result.

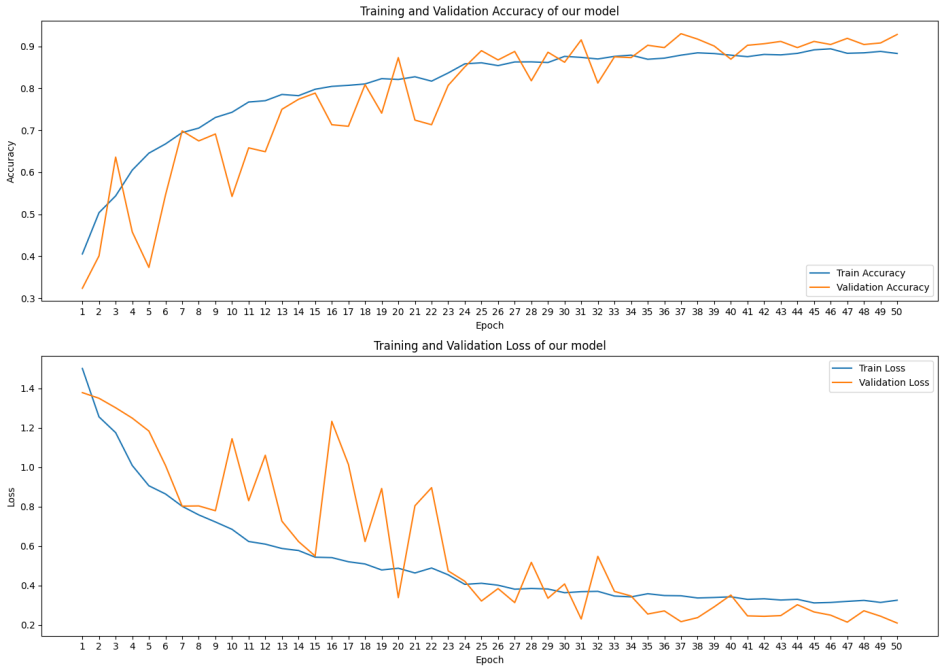

Figure 8: Accuracy and Loss of Training and Validation of Our Model

Table 4: Comparison of different models

Model	**Accuracy**	**Precision**	**Recall**	**F1-score**
VGG16	96%	96%	96%	96%
InceptionV3	97%	97%	97%	97%
Our Model	87%	88%	87%	87%

The performance table reveals that the InceptionV3 model excels with an accuracy, precision, recall, and F1-score of 97%. VGG16 also demonstrates strong performance with corresponding scores of 96% for the metrics.

In contrast, our model, which is a variant of VGG16, achieves lower scores of approximately 87% across all these metrics. Despite this, it's important to highlight that these results are still promising. The decrease in performance could be attributed to factors such as task complexity, data quality, or the specific architecture of our model.

Considering the parameters table, our model has significantly fewer parameters (5M) compared to VGG16 (14M) and InceptionV3 (22M). Despite this, our model still achieves competitive performance, indicating the effectiveness of our model architecture. Potential improvements could be achieved by fine-tuning the model parameters or employing more advanced techniques for feature extraction and classification.

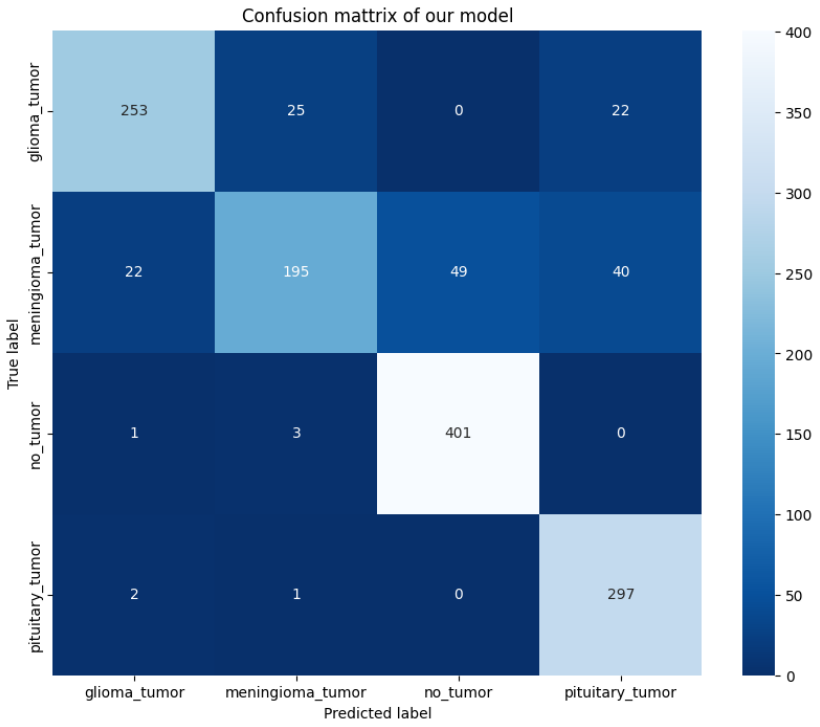

Figure 9: The Confusion Matrix of Our Model

	Precision	**Recall**	**F1-score**	**Support**
gioma_tumor	0.91	0.84	0.88	300
meningioma_tumor	0.87	0.64	0.74	306
no_tumor	0.89	0.99	0.94	405
pituitary_tumor	0.83	0.99	0.90	300

Table 5: Classification Report of Our Model

The confusion matrix above shows that our model performs well for 'Glioma ', 'No Tumor', and 'Pituitary' classes with few misclassifications. However, it struggles with the 'Meningioma' class, often confusing it with 'No Tumor' and 'Pituitary'.

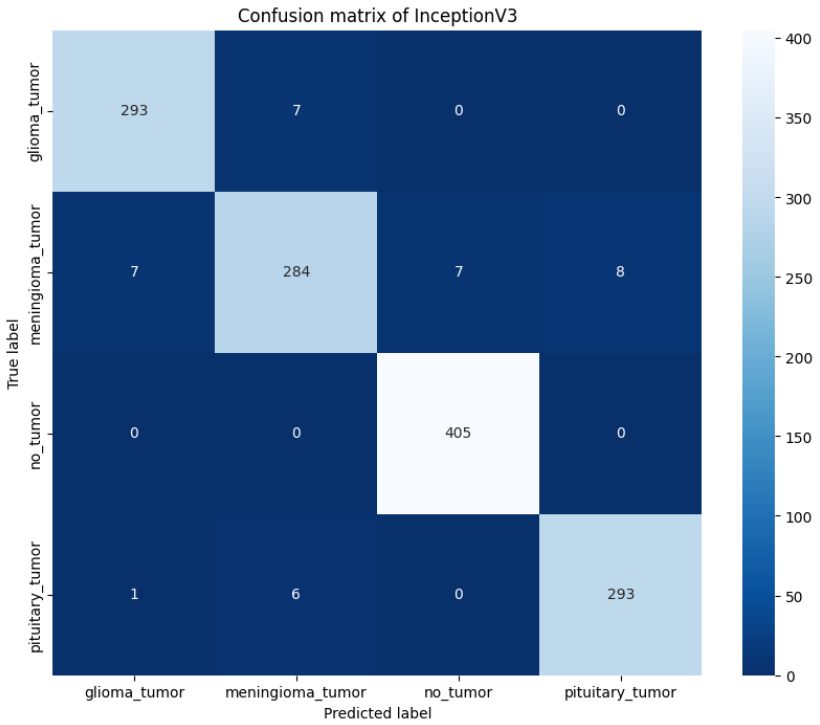

Figure 10: The Confusion Matrix of InceptionV3

	Precision	**Recall**	**F1-score**	**Support**
gioma_tumor	0.97	0.98	0.98	300
meningioma_tumor	0.96	0.93	0.94	306
no_tumor	0.98	1.00	0.99	405
pituitary_tumor	0.97	0.98	0.98	300

Table 6: Classification Report of InceptionV3

InceptionV3 has achieved excellent performance across all classes. It has a minor struggle with 'Meningioma', misclassifying it as 'Glioma' and 'Pituitary'. However, its overall performance is impressive.

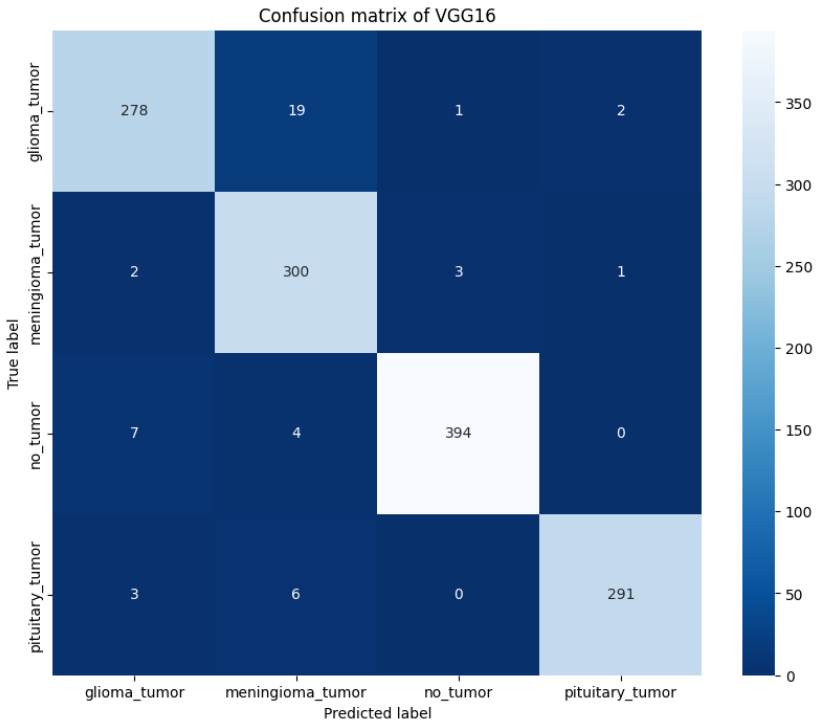

Figure 11: The Confusion Matrix of VGG16

	Precision	Recall	F1-score	Support
gioma_tumor	0.96	0.93	0.94	300
meningioma_tumor	0.91	0.98	0.94	306
no_tumor	0.99	0.97	0.98	405
pituitary_tumor	0.99	0.97	0.98	300

Table 7: Classification Report of VGG16

VGG16 performs well, especially for 'Meningioma' and 'No Tumor'. It has some misclassifications for 'Glioma' and 'Pituitary', indicating room for improvement in these areas.

5.3 Error Analysis

Through analyzing the output of our model, the considerable amount of false predictions for 'Meningioma' as 'No Tumor' or 'Pituitary' could be attributed to several factors. Meningioma is a slow-growing, noncancerous tumor that arises from the meninges, the tissue that covers the brain and spinal cord. It is not considered a type of pituitary tumor, as they arise from different parts of the endocrine system.

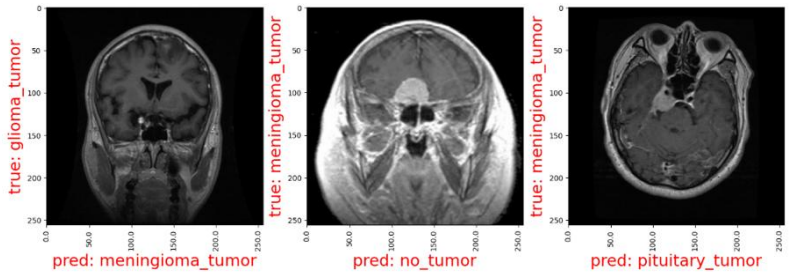

Figure 12: Some cases when our model misclassifies the classes

The misdiagnosis may occur due to the tumor's non-symptomatic nature, or similar presentation to other conditions. Accurate diagnosis of meningioma typically involves imaging studies and specialized testing. However, these nuances might not be captured adequately by the model, leading to misclassification.

Another potential reason could be the use of 2D images in the dataset. The lack of a third dimension could make it challenging for the model to accurately identify the location and extent of the tumor, which are crucial factors in tumor classification.

Additionally, the model might not have seen enough examples of 'Meningioma' in the training data to learn its unique characteristics.

These findings suggest that while our model is generally effective, there is room for improvement, particularly in the classification of the 'Meningioma' class. Future work could focus on gathering more diverse data for 'Meningioma', incorporating 3D imaging data, or fine-tuning the model to better capture the unique characteristics of this class.

5.4 Discussion

Diving into further interpretation, our model and VGG16 are both convolutional neural networks, but they differ in architecture and performance. VGG16, with its 13 convolutional layers, can learn more complex features. This could explain its superior performance compared to ours with 8 convolutional layers.

Our model incorporates more dropout layers and additional batch normalization layers, which are not present in VGG16. These additional layers are beneficial for reducing internal covariate shift and accelerating training but might introduce some noise into the model. Thus, this affects the model's learning ability and results in lower performance. Furthermore, the increased use of dropout in our model, to prevent overfitting, might have led to underfitting.

In short, despite our model sharing several architectural similarities with VGG16, the differences in depth, the use of batch normalization, and the amount of dropout could explain why VGG16 outperforms our model.

6 Conclusion

The effectiveness of several deep learning models in the field of medical image processing has been proven by our study. The VGG16 and InceptionV3 models demonstrated exceptional performance; InceptionV3 achieved an astounding 97% F1-score, accuracy, precision, and recall. Even yet, our suggested model provides a strong foundation for

further improvements, although significantly lagging behind with an 87% score across these measures. This study opens the door for the use of sophisticated machine learning techniques in clinical practice by highlighting their potential to increase diagnostic accuracy. Important insights into the efficacy of the model may be gained by comparing performance indicators including accuracy, precision, recall, F1 score, and error rate.

7 Future works

Future research can investigate several pathways to augment the efficacy and practicality of the models we have suggested. First off, increasing the dataset's size and diversity will be essential to raising the classification's level of accuracy and resilience. Furthermore, exploring algorithm optimization strategies—especially those customized to Our Model's distinct architecture—can improve learning rates and convergence, which will improve the model's performance. Additionally, evaluating the models in real-world clinical situations will highlight any essential feature additions or alterations, as well as offer insightful information about their practical value. Last but not least, a more thorough comparison with other cutting-edge models in the area will allow us to compare the performance of Our Model and confirm its effectiveness in medical picture processing. We want to continuously improve our models' capabilities through these next projects, which will ultimately lead to better patient care and diagnostic accuracy in clinical practice.

Conflicts of Interest: The authors declare no conflict of interest to report regarding the present study.

References

[1] D. Louis, A. Perry, G. Reifenberger, A. Deimling, D. Figarella-Branger, W. Cavenee, H. Ohgaki, O. Wiestler, P. Kleihues, and D. Ellison, "The 2016 world health organization classification of tumors of the central nervous system: A summary," *Acta Neuropathol*, vol. 131, pp. 813–820, 2016.

[2] J. Kang, Z. Ullah, and J. Gwak, "Mri-based brain tumor classification using ensemble of deep features and machine learning classifiers," *Sensors*, vol. 21, p. 2222, 2021.

[3] H. Gao and X. Jiang, "Progress on the diagnosis and evaluation of brain tumors," *Cancer Imaging*, vol. 13, pp. 466–481, 2013.

[4] j. t. y. v. n. p. a. k. d. I. m. Dr. K. KanthammBiB8, author=Yu, Jun and Tan, Min and Zhang, Hongyuan and Rui, Yong and Tao, Dacheng, "Improved clahe enhancement technique for underwater images."

[5] B. Tahir, S. Iqbal, S. Iqbal, M. U. G. Khan, T. Saba, Z. Mehmood, A. Anjum, and T. Mahmood, "Feature enhancement framework for brain tumor segmentation

and classification," *Microscopy Research and Technique*, vol. 82, pp. 803 – 811, 2019. [Online]. Available: https://api.semanticscholar.org/CorpusID:73431303

[6] D. J. Hemanth, C. K. S. Vijila, A. I. Selvakumar, and J. Anitha, "Performance improved iteration-free artificial neural networks for abnormal magnetic resonance brain image classification," *Neurocomputing*, vol. 130, pp. 98–107, 2014. [Online]. Available: https://api.semanticscholar.org/CorpusID:29020239

[7] J. S. Paul, A. J. Plassard, B. A. Landman, and D. Fabbri, "Deep learning for brain tumor classification," in *Medical Imaging*, 2017. [Online]. Available: https://api.semanticscholar.org/CorpusID:64118450

[8] P. Afshar, A. Mohammadi, and K. N. Plataniotis, "Brain tumor type classification via capsule networks," *2018 25th IEEE International Conference on Image Processing (ICIP)*, pp. 3129–3133, 2018. [Online]. Available: https://api.semanticscholar.org/CorpusID:3644467

[9] S. Das, O. F. M. R. R. Aranya, and N. N. Labiba, "Brain tumor classification using convolutional neural network," in *2019 1st International Conference on Advances in Science, Engineering and Robotics Technology (ICASERT)*, May 2019, pp. 1–5.

[10] Y. Liu, M. Muftah, T. Das, L. Bai, K. Robson, and D. P. Auer, "Classificatioo of mr tumor images based on gabor wavelet analysis," *Journal of Medical and Biological Engineering*, vol. 32, pp. 22–28, 2012. [Online]. Available: https://api.semanticscholar.org/CorpusID:60136093

[11] N. Ghassemi, A. Shoeibi, and M. Rouhani, "Deep neural network with generative adversarial networks pre-training for brain tumor classification based on mr images," *Biomed. Signal Process. Control.*, vol. 57, 2020. [Online]. Available: https://api.semanticscholar.org/CorpusID:209926561

[12] J. Sachdeva, V. Kumar, I. Gupta, N. Khandelwal, and C. K. Ahuja, "A package-sfercb-"segmentation, feature extraction, reduction and classification analysis by both svm and ann for brain tumors"," *Appl. Soft Comput.*, vol. 47, pp. 151–167, 2016. [Online]. Available: https://api.semanticscholar.org/CorpusID:43643558

[13] J. Ludzik, A. L. Becker, C. Lee, and A. Witkowski, "Augmenting pigmented lesion assay results with the three-point dermoscopy checklist to improve pigmented lesion triage," *Skin Research and Technology*, vol. 28, pp. 877 – 879, 2022. [Online]. Available: https://api.semanticscholar.org/CorpusID:252541577

[14] A. W. Setiawan, "Effect of color enhancement on early detection of skin cancer using convolutional neural network," *2020 IEEE International Conference on Informatics, IoT, and Enabling Technologies (ICIoT)*, pp. 100–103, 2020. [Online]. Available: https://api.semanticscholar.org/CorpusID:218597927